

# Mesoscale Simulation of Alkali-Silica Reaction

Zarina Itam

**Abstract**— Alkali-silica reaction (ASR) deformation causes a random network of crack patterns on the concrete surface and leaching of the ASR gel. The rapidity of its expansion in an affected structure causes early deformation to the structure, making the understanding of its process a necessity to the engineering field. Factors that affect ASR vary, although it is unanimous that ASR occurs between deleterious silica from aggregates and hydroxide ions in the pore solution that result from cement hydration. Other factors include the relative humidity, temperature and porosity of the cementitious matrix. Temperature influences the kinetics of silica disintegration. Moisture works as a swelling agent for the gel which is hydrophilic in nature. The resultant gel flows into the voids or accumulates on the aggregate surface. The gel expands with the availability of moisture, exerting internal pressure onto the surrounding matrix and lowering the concrete stiffness to the point of cracking. What sets apart ASR with other concrete damage models is its heterogeneity, occurring at different regions at different rates depending on the concrete composition and external influences, making predicting its behaviour difficult. The heterogeneity of the process depends on the pore distribution and the rate of water diffusion. ASR is studied at the mesoscale level to gain an explicit insight on what happens at the material level. Modeling on this level allows the matrix adjacent to the aggregate surface to be developed. This allows us to study the different phases separately, for instance, the effects of ASR gel expansion on the aggregates as well as the bulk matrix. Numerical simulation has enabled us to build models for the representation of different physical phenomena in so many engineering problems. The potential of ASR simulation in detecting the possibility of expansive pressures due to ASR at a fine scale gives new perspective to this phenomenon.

**Index Terms**— Alkali-silica reaction, finite element, material modeling, mesoscale, Newton-Raphson, thermo-chemo-hygral simulation, two-phased material.

## 1 INTRODUCTION

ALKALI-SILICA REACTION (ASR) expansion in an affected concrete structure may happen rapidly and cause deformation to the structure well before its serviceability limit is reached, hence understanding the process is crucial. ASR deformation can be identified by a random network of crack patterns on its surface known as map cracking, leaching of the ASR gel and concrete spalling.

The ASR process occurs when hydroxide ions in the pore solution interact with silica from the aggregates. Hydroxide ions, being alkaline in nature attack the reactive silica sites at the aggregate surface, producing a hydrophilic gel. This gel accumulates at the reaction sites and fills into adjacent voids, replacing the silica it consumed in producing the gel.

When moisture diffuses into the affected concrete, this gel expands and migrates into the connecting porous medium resulting in an internal build up of tensile stresses in the matrix. This will eventually lower the concrete stiffness.

The amount of pressure exerted by the ASR gel expansion varies depending on a number of factors which include the relative humidity, temperature, the type and proportions of reacting materials and gel composition. The most known literatures on ASR are from Dent-Glasser and Kataoka [5], Swamy [14] and Larive [8], which are all referred to in this research.

Previous works for ASR simulation can be found from the works of Capra [3] and Ulm [15], Bazant [2], Bangert [1] and Fairbairn [6]. Li and Coussy [9] developed a thermo-hydro-chemo-mechanical model to study the behavior of ASR affected concrete based on the Biot-Coussy theory on mechanics of

reactive porous medium.

Moranville-Regourd [11] suggested that the use of thermo-dynamics as an irreversible process associated with the continuum damage theory will enable ASR deteriorated zones to be identified. Capra [3] suggested that ASR gel composition is heterogeneous from one reactive site to another, depending on time and the initial content of silica and alkali.

Numerical simulation of stress anisotropy due to ASR is performed by taking into consideration thermoactivation of alkali-silica reactivity and its dependency on relative humidity. The determination of the local ASR reaction extent,  $\xi$  is performed with a stable time integration method, for instance, the Backward Euler method, taking into account the corresponding moisture and temperature profiles for each time step of the numerical procedure. The reaction extent,  $\xi$  is determined from:

$$\xi(t) = \frac{\varepsilon}{\varepsilon_{\infty}} = \frac{1 - \exp(-t/\tau_c)}{1 + \exp(-t/\tau_c + \tau_L/\tau_c)} \quad (1)$$

Where  $\varepsilon_{\infty}$  is the asymptotic ASR expansion.

Ulm [15] defined  $\tau_L$  as the latency time as the time needed for the initial expansion of the gel in the presence of water.  $\tau_c$  is the characteristic time that is defined by the intersection of the tangent at  $\tau_L$  with the asymptotic unit value of the reaction extent,  $\xi$ .  $\tau_c$  and  $\tau_L$  are thermally dependent and can be expressed in terms of absolute temperature ( $TK = 273 + T^{\circ}C$ ) and the corresponding activation energies that abide the Arrhenius concept:

$$\begin{aligned} \tau_L(T) &= \tau_L(T_0) \exp \left[ U_L \left( \frac{1}{T} - \frac{1}{T_0} \right) \right] \\ \tau_c(T) &= \tau_c(T_0) \exp \left[ U_c \left( \frac{1}{T} - \frac{1}{T_0} \right) \right] \end{aligned} \quad (2)$$

• Dr.-Ing. Zarina Itam is currently attached to the Civil Engineering Department of the College of Engineering in Universiti Tenaga Nasional (UNITEN), Malaysia. E-mail: izarina@uniten.edu.my

The variables  $U_L$  and  $U_C$  are the activation energies which represent the minimum energy required to trigger the reaction for the time constants and were determined to be  $U_L = 9400 \pm 500K$  and  $U_C = 5400 \pm 500K$  [2].

The time constants,  $\tau_C$  and  $\tau_L$  tend to have different intensities for drying, sealed, humid and immersed in water conditions, proving that ASR reaction extent is influenced not only by temperature as can be seen in (1), but also by the relative humidity.

Lund [10] stated that the total thermal strain increment could be summed up over the current and history temperature range:

$$\varepsilon_{ij}^{th} = \left[ \int_{T_0}^T \alpha_T (T - T_0) \right] \delta_{ij}. \quad (3)$$

The post-computation of the thermoelastic strain starts with the iteration of (3), resulting in thermal strains,  $\varepsilon^{th}$ . The numerical solution of the equation for temperature  $T + dT$  can be solved using the Backward Euler method:

$$\varepsilon_{ij}^{th}(T + dT) = \varepsilon_{ij}^{th}(T) + \alpha_T(T + dT)dT \delta_{ij}. \quad (4)$$

Where  $\alpha_T$  is a thermal expansion coefficient matrix,  $T$  is the temperature at a given point and  $T_0$  is the temperature at which the structure is free of thermally induced strain.

ASR strain can be represented in an equation for free linear expansion,  $\varepsilon^a$  as shown in (5):

$$\varepsilon^a(t) = \varepsilon_\infty \xi(t). \quad (5)$$

Where  $\varepsilon_\infty$  is the asymptotic ASR expansion. Equation (5) shows that ASR strain evolution is only governed by the non-instantaneous kinetics of the chemical reaction. In a stress-free condition, the only unknown is the reaction extent,  $\xi$ .

The stress states from the mechanical response are obtained from the rheological modeling adding the effect of thermal strain,  $\varepsilon^{th}$ , ASR strain,  $\varepsilon^a$ , pore pressure,  $P^f$ . The constitutive equation can be modified into (6):

$$\sigma = [C(\varepsilon - \varepsilon^a - \varepsilon^{th}) - P^f \mathbf{1}]. \quad (6)$$

Where  $C$  is the fourth order linear elastic material tensor.

## 2 MODELING ASR AT THE MESOSCALE

Material models at the mesoscopic level help to gain insight into the origin and nature of concrete behavior. Previous works on ASR by Ulm [15], Larive [8] and Comi [4] model concrete as a two-phase material which includes the homogenized skeleton with interstitial pores as a phase and the ASR gel as another.

The model presented in this paper is performed at the mesoscale where the model consists of two phases, the aggregates as one phase and the homogenized skeleton with interstitial pores as the other. Although the problems are not examined in full engineering detail, nor is the porosity of the matrix explicitly simulated, the model is sufficient to demonstrate the workability of the algorithm applied in this research.

This has been proven feasible by a series of validation tests conducted with benchmark examples in the following section. Results from the ASR testing in the Finger-Institut Baustoffkunde, Bauhaus-Universität Weimar, Germany will

be numerically simulated and a comparison will be made by means of a mesoscale model of ASR deformation for a heterogeneous concrete prism in order to study the effects of ASR on concrete at the mesoscale.

## 3 METHODOLOGY

### 3.1 ASR Performance Test

There are numerous types of performance tests for alkali-silica reactivity in aggregates, but the tests at the Finger-Institut Baustoffkunde were conducted using the cyclic climate chamber. The performance test by this method is a simplified and time-lapsing simulation of different conditions like drying, moistening and freeze-thawing and their complex interaction [13]. This allows the initiation and acceleration of potential damaging processes in the concrete structure by intensification of transport and reaction processes. It also exposes the tested concrete to in-situ conditions, ensuring optimal exposure to reactants for optimum reaction conditions.

The temperature conditions in the chamber can be set ranging from  $-40^\circ\text{C}$  to  $+90^\circ\text{C}$ . It is also capable of simulating freezing, thawing, fogging and drying conditions. The temperature changing rate is up to 5 K/min. Moisture condition in the chamber ranges from 5% relative humidity to 100% relative humidity. Moistening at 100% relative humidity simulates conditions of fog while drying is simulated at  $<10\%$  relative humidity [13].

QuickTime™ and a decompressor are needed to see this picture.

Figure 1. ASR climate chamber storage cycle [13]

Temperature conditions in the climate chamber follows a 21-day cycle as shown in Fig. 1. Before placing the prisms in the climate chamber, the initial length measurements were taken at  $20^\circ\text{C}$ . Temperature fluctuations from  $5^\circ\text{C}$  to  $65^\circ\text{C}$  are introduced to promote initial cracking. The prisms were then exposed to a drying period of 4 days at  $60^\circ\text{C}$  and a relative humidity of  $<10\%$ .

The temperature is then brought down to  $20^\circ\text{C}$  and measured for length change, after which a fogging temperature will be subjected for 18 days at  $45^\circ\text{C}$  at 100% relative humidity. The prism length change is then measured again at  $20^\circ\text{C}$ . This stage is followed by a period of freezing and thawing for 3 days, at temperature ranging from  $-20^\circ\text{C}$  to

20°C, which is ended by a final measurement of the prism length change [13].

Usual mix proportions are made from a selected ratio of cement/fine reactive aggregate by weight for a specific cement content and water/cement ratio. Specimens will be prepared for ASR mixes with deicing solutions exposed to the top surface, as well as a control mix where just water is exposed to the surface. In order to accelerate the effects of ASR process, ordinary Portland cement with high alkali content is used.

Hobbs [7] proved that rapid and drastic variations of temperature due to seasonal changes are very small and only affect the surface of the structure since change in concrete due to temperature is slow and limited. Plus, ASR deformation may take a long time to evolve. Hence, investigation of the long-term ASR process with a temperature history should be considered. However, due to temporal and financial constraints, this is not always possible. Therefore, the Finger-Institut Baustoffkunde mortar bar tests performed in cyclic chamber gives a faster outlook to the ASR deformation influenced by temperature and moisture in the long-term for an accelerated case.

relative humidity of the prism vary according to experimental setting. The prism is exposed to 8 cycles of the 21-day temperature and humidity fluctuations outlined in Section A, where the model is subjected to drying, fogging, freezing and thawing, and exposed to temperatures ranging from 65°C to -20°C and humidity ranging from <10% to 100% within one cycle [13].

### 3.3 Theories and Assumptions

Since the model is relatively small, the heat and moisture diffusion lengths are found to be constant throughout the prism. Therefore the initial latency and characteristic time constants,  $\tau_L$  and  $\tau_C$  throughout the prism can be taken as constant. The effect of ASR chemical reaction is implemented by using the asymptotic ASR expansion,  $\varepsilon_\infty$  which is determined from inverse analysis from Finger-Institut Baustoffkunde experimental results and taken at an average of 0.22. The values for the modulus of elasticity,  $E$  and Poisson's ratio,  $\nu$  are estimated from experimental results. Other properties were assumed accordingly. This research considers exposure of the prism to water only and no other deicing solution.

As a means of studying the orientation of damage in the matrix and aggregates until fully damaged, the Newton-Raphson iterative method was used. Using this method, the difference between externally applied nodal point loads vector,  $\mathbf{F}_{n+1}$  and the internal node point loads that corresponds to element stresses,  $\mathbf{R}^i$  at iteration step  $i$  must equal to zero as shown in (7):

$$\mathbf{F}_{n+1} - \mathbf{R}^i = 0. \quad (7)$$

Where  $\mathbf{R}^i$  is the vector of internal nodal point loads in the configuration that corresponds to the element stresses at iteration step,  $i$  and  $\mathbf{F}_{n+1}$  is the vectors of externally applied nodal point loads in the configuration at iteration step,  $i$ . More on the Newton-Raphson iteration can be found in literature.

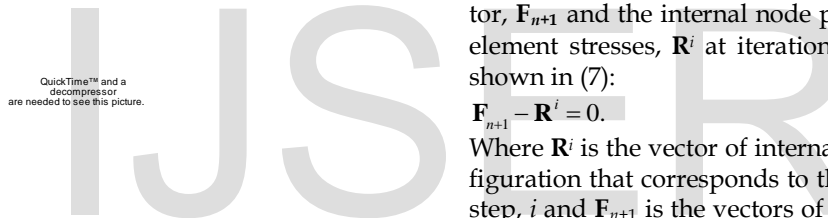


Figure 2. ASR expansion (mm/m) over time (days) for concrete prism exposed to water [13]

An example of ASR gel expansion from mortar bar tests is shown in Fig. 2. According to Stark [13], the limit of expansion for ASR performance test is set to 0.4 mm/m without deicing solution. Aggregates that cause expansion over 0.4 mm/m is considered as reactive. Bangert [1] explains that the volumetric expansion  $\varepsilon_\infty$  is represented with the height of the graph. This parameter is used for an inverse analysis for ASR simulation in the next section.

### 3.2 Modeling Parameters

A two-dimensional mesoscale model of a concrete prism was used for testing measuring 100 mm x 100 mm. The mesoscale model is made up of a two-phased heterogeneous material consisting of aggregates as a phase and the cementitious matrix with interstitial pores as another phase. The mesoscale model is made up of 9651 three-noded plane elements with a total of 28953 nodes as shown in Fig. 3.

The boundary conditions have been set for the effects that are taken into consideration are thermal and moisture fluctuations. The boundary conditions for temperature and

QuickTime™ and a decompressor are needed to see this picture.

Figure 3. Finite element model of the two-dimensional three-noded plane elements mesoscale model of a 100 mm x 100 mm concrete prism

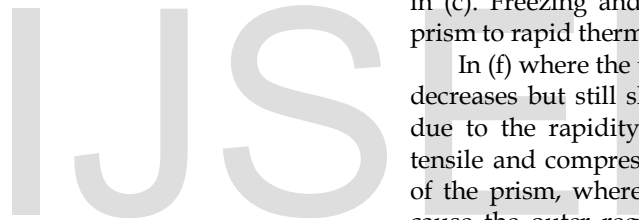
### 3.4 Findings from Simulation

Due to the small prism dimensions with symmetrical results in both the  $x_1$  and  $x_2$  directions, only the  $x_2$  results are discussed in this section. Fig. 4 shows the vertical stress distributions of

the mesoscale models for heterogeneous materials for selective dates within one cycle in the climate chamber. Fig. (a) and (b) show the vertical stress distributions for thermal fluctuations of 60°C and 5°C imposed to promote initial cracking, (c) shows the vertical stress distribution after 4 days of drying at 60°C and <10% relative humidity, (d) shows the vertical stress distribution for measurement condition where the temperature in the chamber is lowered to 20°C, (e) shows the vertical stress distribution at 18 days after fogging at 45°C and 100% relative humidity, (f) and (g) show the vertical stress distributions for freezing and thawing conditions at temperatures ranging from -20°C to 20°C.

The simulation found that the prisms are subjected to both tensile and compressive strains at different regions throughout the prisms depending on the thermal and moisture conditions in the climate chamber. For example, Fig. (a) and (b) show that the prism is subjected to rapid thermal fluctuations ranging from 65°C to 5°C within a short duration. Under high temperature in (a), the prism shows tensile stresses throughout almost the entire prism with the highest values at the prism surfaces due to the immediate exposure to the extreme conditions.

Figure 4. Vertical stress distributions due to ASR and



QuickTime™ and a decompressor are needed to see this picture.

thermal strains of heterogeneous concrete prism for different temperature and relative humidity conditions

The cementitious matrix portrays a lower tensile stress with localized regions of compressive stress, probably a response to the high tensile stress portrayed by the aggregates compressing the matrix that has lower strength. Overall, the prism expands outwards. In (b) where the temperature drops to 5°C, the prism shrinks, causing compressive stresses along the external surfaces. The tensile stress within the prism reduces.

When the prism is subjected to 4 days of drying at 60°C at <10% relative humidity as in (c), the prism expands similarly to (a), but with higher tensile and compressive stresses since the time constraint is longer. Then in (d) where the temperature is reduced to 20°C and the prism elongation is measured, the prism shrinks slightly due to the temperature decrease, causing compressive stresses.

In (e) where the temperature is increased to 45°C and the relative humidity is set to 100% for fogging conditions, after 14 days, the prism once again expands outwards similar to the drying conditions in (c), but with slightly higher stress values. Eventhough (c) has a higher temperature than in (e), the relative humidity which also plays a major role is ASR is higher in (e), subjecting (e) to slightly higher stress values than in (c). Freezing and thawing in (f) and (g) also exposes the prism to rapid thermal changes ranging from -20°C to 20°C.

In (f) where the temperature drops to -20°C, the expansion decreases but still shows tensile stresses at the outer regions due to the rapidity of the thermal fluctuation. The highest tensile and compressive stresses are found in the mid-region of the prism, where while rapid fluctuations of temperature cause the outer regions to have a more transient effect, the internal regions behave more constant. In (g) where temperature increases to 20°C, the stresses also increase.

Fig. 5 compares experimental results for the ASR expansion for concrete prism with results from numerical simulation. While experimental results yield a more fluctuating expansion curve, the numerical simulation results in a smoother curve. Testing with numerous material properties revealed that the ASR expansion model largely depends on how well one can simulate the environmental conditions and many other variables that are almost impossible to replicate explicitly. However, from this simulation it was found that the height of the expansion depends largely on the asymptotic volumetric strain,  $\epsilon_{vol}$ , which is obtained from inverse analysis or can be assumed according to Larive [8] to be within the range of  $0.1 \pm 0.04\%$  to  $0.4 \pm 0.15\%$ .

QuickTime™ and a  
decompressor  
are needed to see this picture.

Figure 5. Results of ASR expansion (mm/m) over time (days) for concrete prism for different values of asymptotic volumetric strains,  $\varepsilon_{\infty}$  from Finger-Institut Baustoffkunde experiment compared to numerical simulation

#### 4 CONCLUSION

The aim of this research was to determine the effects of temperature and relative humidity on ASR expansivity in a concrete structure. This was performed at the mesoscale level in order to determine the ASR expansion mechanism at a more intricate level allowing us to determine its initiation and orientation.

The mesoscale model was developed to have heterogeneous material properties for aggregates and the cementitious matrix. The determination of ASR expansion with inverse analysis from experimental results and application into modeling shows that ASR expansion can be replicated in numerical simulation, provided with the proper material properties and environmental parameters.

ASR has an increased effect due to moisture content. A higher relative humidity increases the characteristic and latency time constants, which means that a shorter time is needed before expansion occurs. As a benchmark unanimous among researchers, a minimum of 60% relative humidity was required for ASR deformation to occur.

Thermal difference leads to tensile or compressive stresses in concrete. Temperature, as well as relative humidity influences the latency and characteristic time constants, which dictate the rapidity of ASR expansion showing its dependency on the heat and moisture diffusion lengths into the structure, rendering heterogeneous values across the cross-section of the structure according to the relative humidity and temperature distribution. Hence, a mesoscopic study proves to be more suitable to evaluate ASR effects on concrete structures.

Therefore it can be concluded that the intensity of alkali-silica reactivity in a concrete structure due to ASR expansion depends on a lot of factors, most importantly the temperature and relative humidity. Other external factors that play an influence on the expansion and orientation of alkali-silica reactivity are the material properties, boundary conditions and if applicable, external loading.

#### ACKNOWLEDGMENT

The highest gratitude to Prof. Dr.-Ing.habil. Jochen Stark and the staff of Finger-Institut Baustoffkunde for the experimental data and Prof. Dr.-Ing.habil. Carsten Könke and the staff of Institut für Strukturmechanik of Bauhaus-Universität Weimar, Germany for their guidance. Thank you to Universiti Tenaga Nasional for the sponsorship for this paper.

#### REFERENCES

- [1] Bangert F., Kuhl D. & Meschke G. (2004). Chemo-Hygro-Mechanical Modelling and Numerical Simulation of Concrete Deterioration Caused by Alkali-Silica Reaction. *International Journal for Numerical and Analytical Methods in Geomechanics*, 28:68-714. John Wiley & Sons Ltd.
- [2] Bazant Z.P. & Steffens A. (2000). Mathematical Model for Kinetics of Alkali-Silica Reaction in Concrete. *Cement and Concrete Research*, 30:419-428. Elsevier Science Inc.
- [3] Capra B. & Bournazel J.-P. Modelling of Induced Mechanical Effects of Alkali-Aggregate Reactions. *Cement and Concrete Research*, Vol. 28, No. 2, pp.251-260. Elsevier Science Inc. (1998).
- [4] Comi C., Fedele R. & Perego U. (2009). A Chemo-Thermo-Damage Model for the Analysis of Concrete Dams Affected by Alkali-Silica Reaction. *Mechanics of Materials*, 41:210-230. Elsevier Ltd.
- [5] Dent-Glasser L.S. & Kataoka N. (1981). The Chemistry of Alkali-Aggregate Reactions. *Proceedings of the Fifth International Conference on Alkali-Aggregate Reactions*, S 252/23, pp. 66.
- [6] Fairbairn E.M.R., Riberio F.L., Toledo-Filho R.D., Lopes L.E., Silvano M.M., Águas M.F.F. & Guedes Q.M. (2004). Smeared Cracking FEM Simulation of Alkali Silica Expansion using a New Macroscopic Coupled Model. *Proceedings of the 12<sup>th</sup> International Conference on Alkali-Aggregate Reaction in Concrete*.
- [7] Hobbs. D.W. (1988). *Alkali-Silica Reaction in Concrete*. American Society of Civil Engineers.
- [8] Larive C., Laplaud A & Coussy O. (2000) The Role of Water in Alkali-Silica Reaction. *11<sup>th</sup> International Conference on Alkali-Aggregate Reaction*. Québec.
- [9] Li K. & Coussy O. (2004). Comprehensive Chemo-Mechanical Modelling of ASR Expansion in Concrete Structures. *Proceedings of the 12<sup>th</sup> International Conference on Alkali-Aggregate Reaction in Concrete*.
- [10] Lund E. (2002). *Short Note on Thermal and Thermo-Elastic Finite Element Analyses*. Aalborg University.
- [11] Moranville-Regourd M. (1997). Modelling of Expansion Induced by ASR - New Approaches. *Cement and Concrete Composites*, 19:415-425. Elsevier Science Ltd. Great Britain.
- [12] Stark J. & Seyfarth S. *Assessment of Specific Pavement Concrete Mixtures by using an ASR Performance-Test*. Bauhaus-Universität Weimar.
- [13] Stark J. (2008). *Alkali-Kieselsäure-Reaktion*. F. A. Finger-Institut für Baustoffkunde. Bauhaus-Universität Weimar.
- [14] Swamy R.N. (1992). *Alkali-Silica Reaction in Concrete*. Blackie & Son Ltd. Glasgow.
- [15] Ulm F.J., Coussy O. Kefei L. & Larive C. (2000) Thermo-Chemo-Mechanics of ASR Expansion in Concrete Structures. *Journal of Engineering Mechanics*, Vol. 126, No.3.